Dynamically Deforming Single Jointed Diver Models Reduce Pinch off Depth

Elizabeth Gregorio, Iftakhar Alam, Elias Balaras, Megan C Leftwich

Dynamically Deforming Single Jointed Diver Models Reduce Pinch off Depth

Elizabeth Gregorio[1,2]†, Iftakhar Alam,[2] Elias Balaras,[2] and Megan C. Leftwich[2]

[1]PMMH, CNRS, ESPCI Paris-PSL, Sorbonne Université, Université Paris Cité, Paris, France

[2]Department of Mechanical and Aerospace Engineering, The George Washington University, Washington, D.C., 20052 USA

(Received xx; revised xx; accepted xx)

Divers reduce visible splash and earn higher scores by performing the rip entry. The diver impacts the water perpendicular to the free surface then roll forward in a somersault as they pass through the interface. This active shape change separates divers from previously studied entry bodies. This paper investigates how this type of dynamic shape change affects the splash production with a single jointed geometrically simplified diver model that turns after impact with the free surface. The impact and splash development is captured with a high speed camera and analyzed for underwater trajectory, pinch off depth, and splash production. The results show that the dynamic shape deformation after impact reduces pinch off depth by nearly half compared to fixed diver models. We demonstrate how their dynamic deformation causes the air cavity to re-attach to the legs of the model. This changes the shape of the trailing cavity from a wedge to an hourglass, and the cavity collapse occurs at the thinnest point. A non-dimensional pinch off depth based on the arm length of the hinged model and the body length of the fixed model shows collapse of the data for all models. Our results illustrate how dynamic deformation during entry changes the essential length for cavity collapse.

1. Introduction

Competitive divers are an entry body, and their impact produces a splash just like other entry bodies that exceed a threshold impact velocity. However, divers earn significantly higher scores when they minimize their splash. The splash produced during the entry event can be broken into two parts: initial jetting and the Worthington jet (Truscott *et al.* 2014). The initial jetting phase begins when the entry body first disrupts the free surface and pushes the water into a jet that rises up around its sides. For divers, this splash is first seen rising around their hands and wrists and continues until their whole body has passed through the surface. While this initial jetting is unavoidable, divers minimize it by keeping their body perpendicular to the surface. If they have not completed their aerial acrobatics before impact, a large asymmetric splash is produced, similar to an oblique entry or a spinning sphere (Bodily *et al.* 2014; Truscott & Techet 2009).

The second phase of the splash, the Worthington jet, is a result of cavity collapse. After an entry body impacts the free surface it can entrain a column of air that remains attached to the projectile and the air above (Wei & Hu 2014). Eventually, this cavity collapses inwards, producing an upward jet (Grumstrup *et al.* 2007; Lee *et al.* 1997; Richardson 1948). The cavity collapse is often called "pinch off" or "deep seal" and the

† Email address for correspondence: elizabeth.gregorio@espci.fr

depth where it occurs strongly correlates with the final jet height (Gekle *et al.* 2009). Minimizing the Worthington jet is necessary for divers, according to the judges' manual, "An exceptionally good entry will result in what is called a rip entry with almost no splash" (FINA Technical Diving Committee 2017-2021 2020). The rip entry describes the sound of tearing paper produced during entry and the particular maneuver that accomplishes it. Brown *et al.* (1984) provides a detailed description of the body position required to achieve a rip entry using a pike save. A diver dynamically changes their body shape while crossing through the free surface, rolling forward as they enter the water, essentially performing a somersault. This dynamic deformation separates divers from previously studied entry bodies. Figure 1 in Gregorio *et al.* (2023) shows how each portion of this pike save corresponds to the phases entry events for a typical entry body.

Shape deformation has yet to be extensively studied in entry body dynamics. Gregorio *et al.* (2023) developed a geometrically simplified diver model that rotates after impact with the free surface. This study shows that the size of the entrained air cavity corresponds to the speed of the model's turn. Their results showed that the hinged models created a lower air cavity, mostly composed of bubbles. This difference compares well with the large groupings of bubbles seen clinging to the arms and upper body of a diver while performing a rip entry. The present study will extend this research to understand how changes in underwater dynamics affect the above water splash.

Divers follow a curved trajectory after impact. This dynamic underwater trajectory has previously been achieved through spin, oblique impact, and uneven hydrophobic coatings. A sphere with an initial spin will create an initial splash that is shaped as an asymmetric wedge. It will follow a curved trajectory after impact that is reflected in the shape of the entrained air cavity (Truscott & Techet 2006). A symmetric slender body that obliquely impacts the surface will also create an asymmetric initial splash and entrained air cavity (Bodily *et al.* 2014). Additionally, spheres and symmetric slender bodies that have been coated half hydrophobic and half hydrophilic achieve a similar curved trajectory. These entry bodies also create asymmetric initial splashes and entrained air cavities similar to objects given an initial spin or that have an oblique entry (Truscott & Techet 2009; Bodily *et al.* 2014). Divers are also using the rip entry to drastically decelerate during entry. A recent study of divers performing feet first entries showed that they decelerate from their impact velocity to rest within 6 m of the free surface (Guillet *et al.* 2020). Divers and other biological entry bodies, like birds, have a large enough aspect ratio for the air cavity to re-attach to their body during impact (Guillet *et al.* 2020; Chang *et al.* 2016). The effects of deceleration during entry have been thoroughly studied for spheres with different density ratios. Such a sphere will decelerate and even reverse direction during the entry event allowing the sphere to interact with and change its entrained air cavity, both after and before cavity collapse (Aristoff *et al.* 2010).

Finally, divers that are performing an underwater save are essentially performing a somersault; therefore undergoing an asymmetric shape change. Previously studied shape changes in entry body dynamics have largely been symmetric and harmonic. An elastic sphere that impacts the free surface will flatten into a more egg-like shape during impact and then oscillate between that shape and a sphere during the entry event. Hurd *et al.* (2017) shows that while this oscillation changes the shape of the entrained air cavity, the entry event still largely mirrors that of a rigid sphere. Antolik *et al.* (2023) performed experiments with a symmetric slender body whose nose is attached with a compliant flexure springs that approximate a simple harmonic oscillator. They find that it is possible to both reduce and amplify the force with this type of dynamic deformation. The results presented in their study do not indicate any substantial changes to the splash phases during the entry event due to the dynamic shape change.

This study will investigate the mechanism that allows competitive divers to reduce their visible splash by performing the rip entry. It builds on the research presented by Gregorio *et al.* (2023) which shows how a dynamically deforming single jointed diver model changes the formation of the entrained air cavity. The experimental methods used in this study will be explained in Section 2. This includes the geometrically simplified single jointed diver, the method of guided free fall, and the method of tracking to collect the results. The results of these experiments will be presented and discussed in Section 3. Finally, a summary of the results and our conclusions will be presented in Section 4.

2. Experimental Methods

Competitive divers perform the rip entry after a hands first entry from heights below 14 m (Pandey *et al.* 2022). In international competition this includes the 1 and 3 m springboards and 10 m platform. Guillet *et al.* (2020) reports their impact velocity from these heights as $5.76 - 14.21$ m/s. The relevant non-dimensional numbers for this type of entry body are the Reynolds, $Re = ul/\nu$, Weber, $We = \rho u^2 l/\sigma$, and Froude, $Fr = u/\sqrt{gl}$ numbers (where ρ and ν are the fluid density and kinematic viscosity respectively, g is the acceleration of gravity, σ is the surface tension, and l and u are characteristic length and velocity scales). If we use the height of the diver (2 m) as the characteristic length and the impact velocity above as characteristic velocity we find: $1.11 \times 10^7 < Re < 2.74 \times 10^7$, $0.89 \times 10^3 < We < 2.19 \times 10^3$, and $1.4 < Fr < 3.46$. Therefore, the rip entry is performed in an inertial regime where the external field and length scale has a larger effect on the overall dynamics in ballistic entry. The experimental method developed for this study creates conditions within this same regime for the simplified diver model.

The single jointed diver model is designed to perform a dynamic shape change after impact similar to the somersault performed during a rip entry. Each hinged model consists of two rigid parts 3D printed by a Markforged Desktop 3D printer (Watertown, MA), painted, and connected with a spring pin at the joint. The lower part that impacts the water first is called the arms and the upper part that is fixed to the driving rod is called the legs. The arms have two symmetric cuts and one asymmetric wedge to mimic the hand hold of a diver. A comparison of this simplified diver model alongside a diver in the entry pose can be found in Gregorio *et al.* (2023). Four variations of the asymmetric wedge angle are investigated in this study and each model has a fixed counterpart. The fixed version of this diver model has the same full body length as the hinged model but it is rigid and does not change shape after impact. A sketch of these two simplified diver models can be seen in Figure 1. The four variations of the asymmetric angle include 28.6°, 22.7°, 17.4°, and 10.4°. The naming convention employed in this paper refers to each model with the size of the asymmetric angle and a letter to distinguish between the hinged models (H28, H22, H17, H10) and the fixed models (F28, F22, F17, F10).

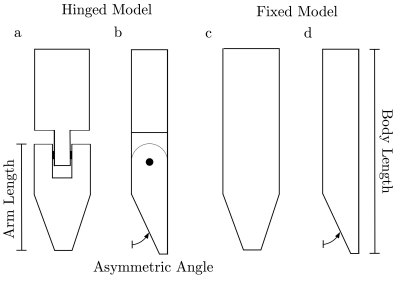

FIGURE 1. Geometrically simplified diver model: a-b) single jointed (H22) c-d) fixed (F22), with 22.7° asymmetric angles labeled.

The diver model is driven into a pool of water using a dropping cage ($2.4 \times 0.9 \times 0.9$ m) constructed around a water tank ($1.2 \times 0.51 \times 0.51$ m). The model is affixed to the center of a cross bar mounted to two gliders to produce a guided free fall. While there is minimal

friction, it does vary between trials which resulted in a range of impact velocities. An IDT NX3S3 (Pasadena, CA) high speed camera is positioned perpendicular to the water tank level with the free surface. The field of view is illuminated from behind by an LED light panel directly across from the camera. The diver model is positioned with its plane of rotation parallel to the light panel and plane of view. Gregorio *et al.* (2023) provides a detailed explanation.

All captured frames where the diver model is visible are tracked using DLTdv8 (Hedrick 2008). During the above surface approach the location of the hands are tracked as seen in Figure 2a. The location of the feet are tracked in every frame where they are visible, above and below the surface (Figure 2b). The moment of pinch off is marked as well as 30 frames of the upward movement of the cavity after cavity collapse (Figure 2c). The angle of deformation is measured for the hinged models 0.0234 s after impact. The height of the splash is measured for all trials 0.0702 s after impact (Figure 2d).

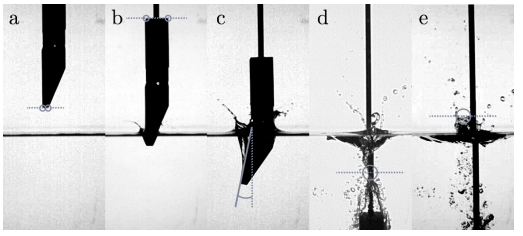

FIGURE 2. Demonstration of tracking locations on a trial for the H22: a) hands, b) feet, c) angle of bend measured at 0.0234 s, d) pinch off, e) splash height measured at 0.14 s

The impact velocity is determined by a linear interpolation of the last 20 tracked points for the hands before impact. We report experiments with impact velocities between 2.1 and 4.5 m/s which gives $3.1 \times 10^5 < Re < 6.6 \times 10^5$, $0.91 \times 10^4 < We < 4.2 \times 10^4$, and $1.76 < Fr < 3.75$. This places these experiments within the same inertial regime as the rip entry. Each trial is identified by its model naming convention and Froude number because Fr reflects the impact velocity and length scale.

3. Results and Discussion

Competitive divers attribute their ability to reduce the visible splash produced by a dive to a properly performed rip entry. This visible splash is the Worthington jet, generated by the inward collapse of the entrained air cavity. Air cavity collapse is commonly called pinch off or deep seal, and the depth where it occurs is related to the final splash height (Gekle *et al.* 2009). Therefore, if the dynamic shape change involved in the rip entry changes an essential part of this air cavity collapse, it would reduce the visible splash. The results presented here will address this question.

Figure 2d demonstrates how the depth of pinch off was marked for each case at the moment of cavity collapse. The amount of time that passed between impact and pinch off is plotted against the Froude number in Figure 3a. There is a small spread in the time of pinch off for both the fixed models (0.02 s) and the hinged models (0.04 s). This aligns with results of previous studies such as the one by Glasheen & McMahon (1996) which notes that the time of pinch off is "nearly independent of velocity." This result shows that the time of pinch off is also nearly independent of dynamic deformation during impact. The depth of pinch off is plotted against the Fr for all trials in Figure 3c. This shows a correlation between the depth of pinch off with Fr for both fixed and hinged models. We see a weak linear correlation between the depth of pinch off and the Fr across models. The fixed models tend to have a deeper pinch off than the hinged models for the same Fr. This indicates that dynamic deformation during the entry event does cause a change in pinch off location. Figures 3a, c and d indicate the R-squared (R^2) value which is a

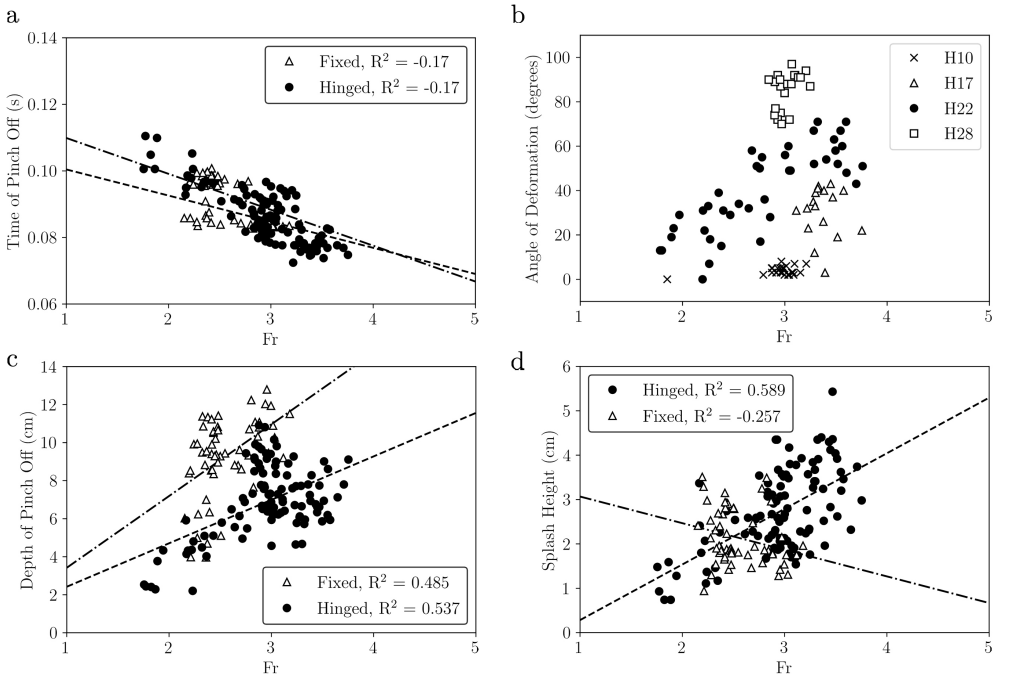

FIGURE 3. Dependence of measured quantities on Froude number ($Fr = u/\sqrt{gl}$): a) time of pinch off (s), b) angle of deformation at 0.0234 s, c) depth of pinch off (cm), d) splash height (cm)

measure of the linear correlation between the two plotted variables and values closer to 1 indicate a stronger linear correlation.

To characterize the difference in dynamic deformation between each trial the angle of rotation was measured at 0.0234 s after impact, shown in Figure 3b. Gregorio *et al.* (2023) fully characterized the deformation of single jointed diver models at a single impact velocity (3.11 ± 0.053 m/s). Under these conditions the dynamic deformation is dependent on the size of the asymmetric wedge and hinge stiffness because the model turns after a sufficient force is applied to the arms. In this study we consider a wider range of impact velocities and Figure 3b shows a linear correlation for the deformation of H22 with impact velocity ($R^2 = 0.804$). The other three models (H10, H17, H28) do not have a strong linear correlation. This means H22 is more sensitive to a change in impact velocity. The deformation of the H10 seems to be particularly independent of the impact velocity across the twenty-five trials shown here. The H17 and H28 show a wide range of angles measured at a single impact velocity which indicates less sensitivity to impact velocity and more sensitivity to hinge stiffness.

The splash height measured 0.14 s after the diver model impacted the free surface is shown in Figure 3d. There is a weak linear correlation between the splash height and the Fr that is more significant for the hinged models. There is a positive linear correlation between splash height and Fr for hinged models. This may result from the similar dynamic deformation performed after impact. Whereas the fixed models do not deform after impact, therefore, the difference in frontal geometry may play a larger role in creating the shape of their entrained air cavity. While these results are interesting, the driving rod required to ensure the feet remain perpendicular to the free surface throughout impact makes it difficult to accurately measure the final splash height. Therefore, we will focus on pinch off depth when comparing the splash production of these diver models.

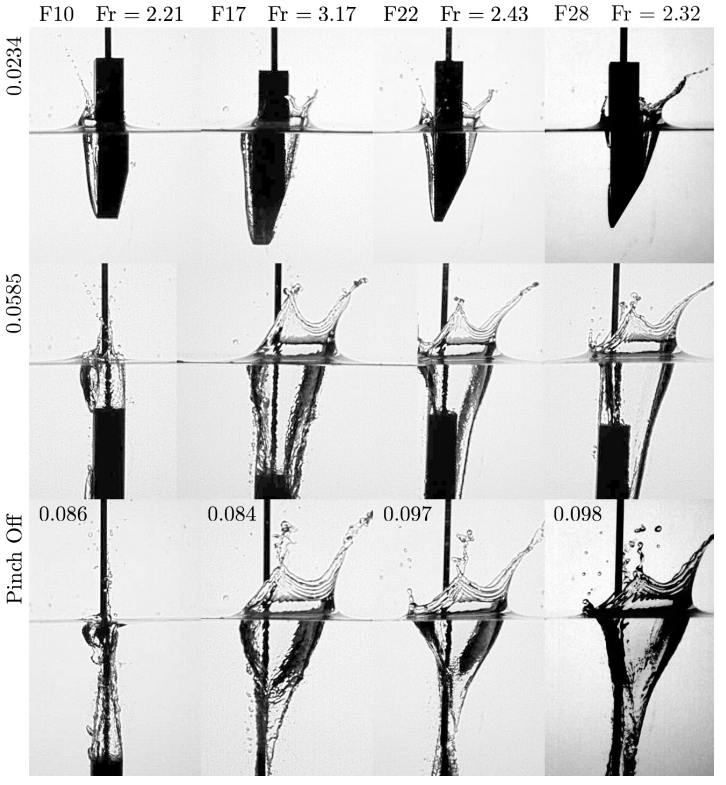

FIGURE 4. Frames from the impact of one example trial for each of the four variations of asymmetric wedges of the fixed diver models.

Changing the asymmetric angle of the diver models creates a different frontal geometry which can affect the entry event (Bodily *et al.* 2014). The influence of frontal geometry is more clear in the results for the fixed models, Figure 4 shows an example impact for each fixed model. In the first frame (0.0234 s), we see that models F17 – 28 have entrained air to the right of the arms while F10 does not. This difference allows for the air cavity to attach to the legs on both sides of F10 at 0.0585 s. While the air cavity entrained by models F17 – 28 is only attached to the left side of the legs and has a wedge shape with a wider opening at the surface. This is one consequence of frontal geometry that creates a clear pinch off depth difference between F10 and F17 – 28.

The influence of dynamic deformation is clear when comparing the impact of F22 and H22 at Fr = 2.43 shown in Figures 4 and 5. The full time series of the impacts are included in supplementary material. The dynamic deformation of H22 begins after impact and allows the air cavity to re-attach to the legs of the model creating an hourglass shaped air cavity at 0.0468 s in Figure 5. F22, on the other hand, has a wedge shaped air cavity that does not fully re-attach to the legs until just before pinch off. The pinch off for each of these entry events shows a visible difference of 5.41 cm between the depth of air cavity collapse. This is consistent with the overall result that hinged models have a shallower pinch off than fixed models for the same Fr (Figure 3c). In fact, this example shows that the cavity collapse for H22 happens at nearly half the depth as F22 when Fr = 2.43.

Figure 3b indicates that the deformation of H22 is particularly dependent on the Fr. This influence is clear in the first row of Figure 5 which shows four examples of H22 entry events in which the Fr and amount of deformation increases from left to right.

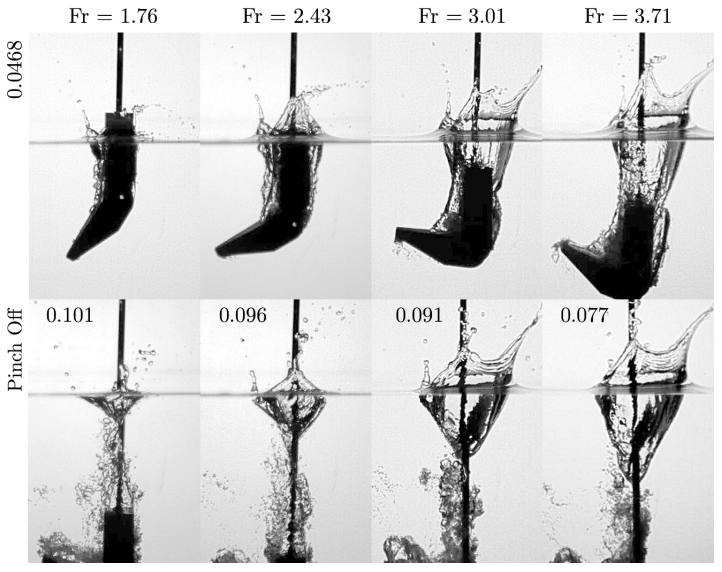

FIGURE 5. Example entry events for H22 at four different Froude numbers increasing from left to right, shown at 0.0468 s after impact and at the moment of pinch off

Only the H22 with Fr = 3.71 has completed its deformation by 0.0468 s. This shows that the difference measured at 0.0234 s continues throughout the entry event. The second row of Figure 5 shows that pinch off time and pinch off depth increases from left to right $(2.54, 5.11, 6.19, 7.80$ cm). There is a 71% difference between largest and smallest Fr and a 102% difference between the shortest and tallest pinch off depth.

The dynamic deformation of the H22 models allows for the air cavities to re-attach to the legs as seen at 0.0468 s in Figure 5. This re-attachment gives the air cavity an hourglass shape, with a thinner portion separating the cavity surrounding the diver model and the portion at the surface. This is one factor that may influence the depth of pinch off which is most clear for Fr = 3.01 and 3.71 which seem to experience pinch off at the center of their hourglass shape. This may stem from a change in hydrostatic pressure gradient inside the cavity due to the hourglass shape and shows that the depth at which the air cavity re-attaches to the legs influences the depth of pinch off.

Differences in frontal geometry as well as rate of deformation influence the entry event for the hinged models. This can be seen in the entry events of each of the studied asymmetric wedges studied at similar Fr's in Figure 6. This figure also shows an increase in completed deformation from left to right, which in this case is caused by the increasing size of the model's asymmetric wedge. We see that the air cavity has re-attached to the legs of all four models by 0.0468 s after impact. The hourglass shape is clearest for H22 and H28 because their dynamic deformation is the furthest along. The pinch off times are within a range of 0.013 s and the pinch off depths are within a range of 2.71 cm. The deepest location of pinch off is for H10 and the shallowest is for H22. H10 has barely deformed at 0.0468 and thus entrains an air cavity with more of a column shape instead of an hourglass shape. This difference likely contributes to the greater pinch off depth. The small range of pinch off depths for models H17 – 28 show that creating the hourglass shape is more important to decreasing pinch off depth than the speed at which the model completes its full deformation.

The results for the fixed and hinged models shown in Figures 4, 5, and 6 show that the hinged diver model typically experiences pinch off at nearly half the depth of the

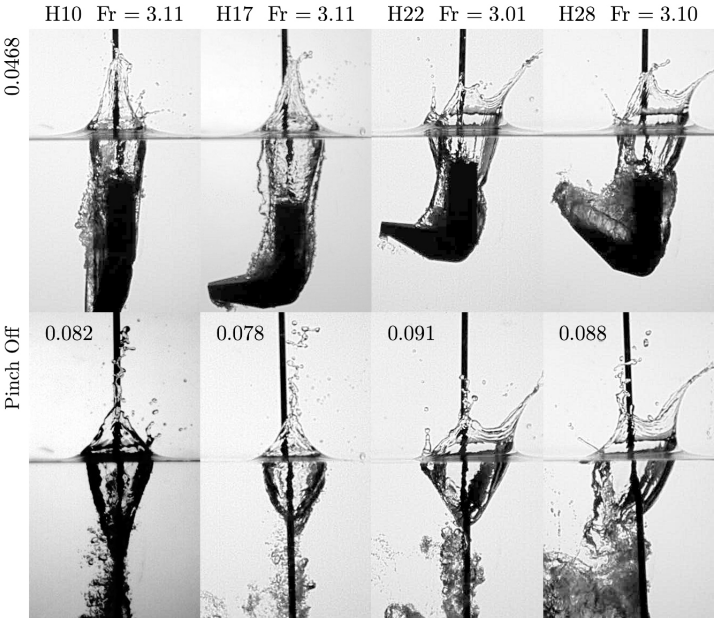

FIGURE 6. Example entry events for each of the four different variations of asymmetric wedges for the single jointed diver model shown 0.0468 s after impact and at the moment of pinch off.

fixed models at the same Fr. With the results for H10 and F10 being an exception to this observation. Figure 1 shows that the arm length of the hinged model is roughly half of the diver's body length. Therefore, it could be useful to develop a non-dimensional pinch off depth based on these two characteristic lengths. We will define this non-dimensional pinch off depth as:

$$D^* = d_{po}/L \tag{3.1}$$

Where d_{po} is the depth of pinch off and the length scale (L) corresponds with the arm length (7.88 cm) for the hinged model and the body length (14.4 cm) of the fixed model. This equation is applied to the data and the result can be seen in Figure 7a. Figure 7b presents a comparison with data found in the literature, in this case D^* is computed with the relevant length scale (L) for the impactors, using diameter for the spheres and length for the axi-symmetric elongated bodies. Figure 7a shows that the pinch off depth results for the present study collapse for both the fixed and hinged models with D^*. The lines of best fit are significantly closer in Figure 7 than Figure 3. In fact, the percent difference in the slope collapses from 48% to 11%. This shows that the dynamic deformation changes the essential length for air cavity creation by allowing for re-attachment to the legs. The model proposed by Gekle *et al.* (2009) shows that the depth of pinch off is directly related to the final height of the splash. Therefore, this significant relationship between L and pinch off depth will likely decrease the final splash for the hinged models.

Previous studies have also investigated the dependence of pinch off depth on Froude number, three of which are included in Figure 7. The data taken from Yan *et al.* (2009) and Duclaux *et al.* (2007) shows a linear relationship for spheres with different diameters and mass ratios. Yan *et al.* (2009) presents an interpolation of this linear realtionship that shows the spheres are predicted to have a greater D^* than the diver models at the

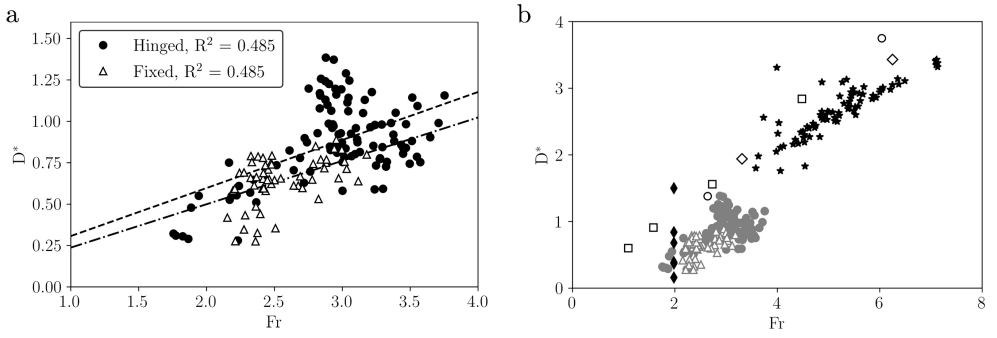

FIGURE 7. Dependence of D^* on Froude number for: a) present data and b) present data (gray) compared to the literature: Bodily *et al.* (2014) axi-symmetric elongated bodies L = 25.4 cm (◆), Duclaux *et al.* (2007) spheres D = 12 mm (○), D = 15.6 mm (◇), D = 24 mm (□), Yan *et al.* (2009) sphere D = 5.72 cm (⋆)

same Fr. Bodily *et al.* (2014) presents an analysis of axi-symmetric elongated entry bodies which are the most similar to the simplified diver models. Their data for hydrophilic and hydrophobic entry bodies with three different nose shapes are included in Figure 7. It is particularly notable that while each data point represents an entry body with different characteristics, the D^* range is the same for these six at one Fr as all data presented for the simplified diver models. Figure 7 shows that in general elongated bodies can decrease D^* in comparison to spheres.

4. Conclusions

Competitive divers use the rip entry to reduce the visible splash produced by a dive. The final splash height, or Worthington jet, is directly related to the depth of pinch off. We used a single jointed diver model that dynamically deforms after impact to identify how the rip entry changes the entry event. Our results indicate that the active shape change modifies the characteristic length for air cavity collapse. When the hinged models deform, the air cavity re-attaches to the legs of the model. This creates an hourglass shaped air cavity and appears to change the hydrostatic pressure gradient that induces cavity collapse. This contrasts with the fixed diver models (F17 – 28) which do not have the same re-attachment and create a wedge shaped air cavity with a deeper pinch off.

The difference in pinch off depth between fixed and hinged models appears to be nearly half, a similar ratio as the arm length to full body length of the geometrically simplified diver models. To investigate this we develop D^*, a non-dimensional pinch off depth based on the two characteristic lengths (L), which collapses our data for all models. This non-dimensional pinch off also allows us to compare our data with what is reported in the literature. The results reported by Bodily *et al.* (2014) for axi-symmetric elongated entry bodies also collapse onto our data when plotted with our D^*. We see that the results for entry bodies with larger aspect ratios experience pinch off at a consistently smaller D^* than spheres (Duclaux *et al.* 2007; Yan *et al.* 2009).

Our results demonstrate how a dynamically deforming slender object changes the entry event. As the object changes shape, the point where the air cavity attaches to the entry body shifts. This changes the depth of pinch off and, therefore, the splash. In this way, the dynamic change in aspect ratio changes the length scale that dominates the splash formation mechanism. These results help to explain why competitive divers are able to use the rip entry to reduce their visible splash to achieve higher scores.

REFERENCES

Antolik, John T, Belden, Jesse L, Speirs, Nathan B & Harris, Daniel M 2023 Slamming forces during water entry of a simple harmonic oscillator. *Journal of Fluid Mechanics* **974**, A23.

Aristoff, Jeffrey M, Truscott, Tadd T, Techet, Alexandra H & Bush, John WM 2010 The water entry of decelerating spheres. *Physics of Fluids* **22** (3), 032102.

Bodily, Kyle G, Carlson, Stephen J & Truscott, Tadd T 2014 The water entry of slender axisymmetric bodies. *Physics of Fluids* **26** (7), 072108.

Brown, Janet G, Abraham, Lawrence D & Bertin, John J 1984 Descriptive analysis of the rip entry in competitive diving. *Research Quarterly for Exercise and Sport* **55** (2), 93–102.

Chang, Brian, Croson, Matthew, Straker, Lorian, Gart, Sean, Dove, Carla, Gerwin, John & Jung, Sunghwan 2016 How seabirds plunge-dive without injuries. *Proceedings of the National Academy of Sciences* **113** (43), 12006–12011.

Duclaux, V, Caillé, F, Duez, C, Ybert, C, Bocquet, L & Clanet, C 2007 Dynamics of transient cavities. *Journal of Fluid Mechanics* **591**, 1–19.

FINA Technical Diving Committee 2017-2021 2020 *FINA Diving Officials Manual*. Fédération Internationale de Natation.

Gekle, Stephan, Gordillo, José Manuel, van der Meer, Devaraj & Lohse, Detlef 2009 High-speed jet formation after solid object impact. *Physical review letters* **102** (3), 034502.

Glasheen, JW & McMahon, TA 1996 Vertical water entry of disks at low froude numbers. *Physics of Fluids* **8** (8), 2078–2083.

Gregorio, Elizabeth, Balaras, Elias & Leftwich, Megan C. 2023 Air cavity deformation by single jointed diver model entry bodies. *Experiments in Fluids* **64** (168).

Grumstrup, Torben, Keller, Joseph B & Belmonte, Andrew 2007 Cavity ripples observed during the impact of solid objects into liquids. *Physical Review Letters* **99** (11), 114502.

Guillet, Thibault, Mouchet, Mélanie, Belayachi, Jérémy, Fay, Sarah, Colturi, David, Lundstam, Per, Hosoi, Peko, Clanet, Christophe & Cohen, Caroline 2020 The hydrodynamics of high diving. *Multidisciplinary Digital Publishing Institute Proceedings* **49** (1), 73.

Hedrick, Tyson L 2008 Software techniques for two-and three-dimensional kinematic measurements of biological and biomimetic systems. *Bioinspiration & biomimetics* **3** (3), 034001.

Hurd, Randy C, Belden, Jesse, Jandron, Michael A, Fanning, D Tate, Bower, Allan F & Truscott, Tadd T 2017 Water entry of deformable spheres. *Journal of Fluid Mechanics* **824**, 912–930.

Lee, M, Longoria, RG & Wilson, DE 1997 Cavity dynamics in high-speed water entry. *Physics of Fluids* **9** (3), 540–550.

Pandey, Anupam, Yuk, Jisoo, Chang, Brian, Fish, Frank E & Jung, Sunghwan 2022 Slamming dynamics of diving and its implications for diving-related injuries. *Science Advances* **8** (30), eabo5888.

Richardson, EG 1948 The impact of a solid on a liquid surface. *Proceedings of the Physical Society* **61** (4), 352.

Truscott, Tadd T, Epps, Brenden P & Belden, Jesse 2014 Water entry of projectiles. *Annual Review of Fluid Mechanics* **46** (1), 355–378.

Truscott, Tadd T & Techet, Alexandra H 2006 Cavity formation in the wake of a spinning sphere impacting the free surface. *Physics of Fluids* **18** (9), 091113.

Truscott, Tadd T & Techet, Alexandra H 2009 A spin on cavity formation during water entry of hydrophobic and hydrophilic spheres. *Physics of Fluids* **21** (12), 121703.

Wei, Zhaoyu & Hu, Changhong 2014 An experimental study on water entry of horizontal cylinders. *Journal of Marine Science and Technology* **19** (3), 338–350.

Yan, Hongmei, Liu, Yuming, Kominiarczuk, Jakub & Yue, Dick KP 2009 Cavity dynamics in water entry at low froude numbers. *Journal of Fluid Mechanics* **641**, 441–461.